Slip Condition Investigation in Textured Surfaces with Transient Elastohydrodynamic Lubrication

Javad Sharifi Yalameh [1], Amir Torabi[2*]

[1]MSc student, Department of Technology and Engineering, University of Shahrekord, Shahrekord, Iran
[2]Associated Professor, Department of Technology and Engineering, University of Shahrekord, Shahrekord, Iran, Email: torabi@sku.ac.ir

Abstract:

The no-slip condition is an accepted condition in common fluid dynamics applications. In some cases, when high speed and pressure occur in a flow region near the surface, such as the lubrication of non-conformal surfaces, this assumption becomes controversial and the observation shows that the fluid can slide on the surfaces. This study has numerically investigated the effect of fluid slippage on the textured surface in transient elastohydrodynamic lubrication. The finite difference method extracted and discretized a numerical transient model based on the Newtonian lubricant fluid flow equations. The flow is assumed isothermal for a geometry including an upper cylinder and a lower flat dimple textured surface. A newly developed precise transient model is used for lubricated contact of a dimpled flat surface and a cylinder. This model considers passing the cylinder over a dimple in several time steps. In this paper, the model is comprehended by the critical shear stress model to consider boundary sliding. The results showed that with slippage, the lubrication friction decreases compared to the no-slip condition estimations. The occurrence of slip causes an average 15.42% decrease in the friction coefficient for flat surfaces. For dimpled surfaces, the occurrence of sliding for different depths of dimples is on average 15% decrease in the amount of friction coefficient while it decreases about 12% for different radii of the dimple.

Keywords:

Slip condition, Friction, Dimple, Critical shear stress, Lubrication

1. Introduction

The assumption of a no-slip surface in the vicinity of the moving surface, which was first presented by Newton, is widely accepted in the fluid dynamics analysis; Contrary to the widespread use of this assumption, in experiments, boundary slip has been observed and reported in several cases such as polymeric flow, corner flow, hydrodynamic lubrication, and especially elastohydrodynamic lubrication [1]. The influencing factors in the elastohydrodynamic lubrication regime are the elastic deformation of the surfaces due to the pressure caused by the applied load over the lubricant film between the surfaces, as well as the large change in the viscosity of the lubricant with pressure. Therefore, it is known as elastohydrodynamic lubrication.

Advances in nanoscale measurements have made it possible for scientists to observe boundary sliding. Wong et al. [2] have provided evidence of lubricant sliding on the steel contacting surface with elastohydrodynamic lubrication in the laboratory. Ponjavic and Wong [3] experimentally argued that the thickness of the film decreases due to the pressure of the flow, and due to the reduction of the shear stress, the friction decreases, ultimately leading to sliding on the contact surface. Guo et al. [4] have investigated and tested the relationship between contact hysteresis angle and hydrodynamic lubrication of a sliding bearing. The contact angle is related to the force of attraction between the molecules in the contact interface of solid and fluid, and in this way, it can affect the possibility of sliding at the interface. Jin et al. [5] have tested and researched the changes of the lubricant film in reciprocating motion with zero entry speed. The results showed the dependence of slip on transient and load effects. Feng et al. [6] investigated the hydrodynamic performances of partial microgroove water-lubricated bearings considering the partial wall slip. The results show that wall slip can enhance the load capacity. Tauviqirrahman et al. [7] studied the thermo-hydrodynamic characteristics of heterogeneous slip/no-slip bearings running under steady, incompressible, and turbulent conditions. They showed that the load-carrying capacity of the heterogeneous slip/no-slip bearing can be significantly increased by up to 100% depending on the rotational speed. Arif et al. [8] conducted a study for the suitable location of slip boundary conditions and microscale surface

textures to enhance the tribological performance of the hydrodynamic journal bearings. Arif et al [9] indicate that the combined effect of slip boundary condition and micro-texture with a suitable selection of lubricant rheology is beneficial in increasing the stability of hydrodynamic lubricant film in the journal bearings. Yao et al. [10] indicated the positive effect of the wall slip on the transient hydrodynamic performance of water-lubricated bearing is highly dependent on the eccentricity ratio, and that the maximum slip velocity is more affected by the slip region compared with the minimum slip velocity. Yi et al. [11] showed that the friction coefficient increases first and then decreases with thickening water film, while the slip length have a contrary change.

In some studies, due to observing a difference in bearing performance in the case of slip occurrence in contacting surfaces, they have presented a theoretical model for lubrication analysis. They also use popular numerical methods such as finite elements for these problems. Zhang and Wen [12] have studied the isothermal contact line of elastohydrodynamic lubrication between a cylinder and a perfectly flat plate under different slip-to-roll ratios and using the shear stress slip model. Their results showed that the interfacial limiting shear stress effect can directly cause a drastic film thickness reduction. Aurelian et al. [13] have presented a finite element method to investigate the effect of wall slip on elastohydrodynamic journal bearing. In this work, the combined effect of surface pattern and slip has been studied and by comparing the load carrying capacity and load loss, it has been shown that by choosing a suitable pattern for the surface, the performance of the bearing can be effectively improved. Chen et al. [14] have studied the effects of anisotropic sliding on elastohydrodynamic lubrication. Their results showed that the film thickness is more sensitive to the slip length in a sliding direction (x-direction) than to the slip length in a transverse direction (y-direction). Zhao et al. [15] have presented a linear complementary solution for two-dimensional elastohydrodynamic lubrication contact boundary sliding. This numerical solution has been done for point contact of elastohydrodynamic lubrication under isothermal conditions and pure rolling. Sun et al. [16] have investigated the effect of local boundary sliding on increasing load-carrying capacity. Experimental evidence has been obtained by the sliding test device on the optical disk. Numerical analysis

of the sliding effect has been carried out using the limit shear stress model and with the help of the modified Reynolds equation for hydrodynamic lubrication to determine the load-carrying capacity. The results of the numerical analysis and the data obtained from the experiment have stated that the appropriate sliding pattern on the fixed surface of the bearing can improve the load-carrying capacity. Cam et al. [17] considered the wall slip and cavitation in the lubrication. They introduced a model for the slippage at the wall is proposed by modifying the multi-linearity wall slip model to improve accuracy and computational cost.

As the review of studies shows, the issue of fluid sliding on the surface in lubrication conditions can cause many common estimates to be wrong. On the other hand, the development of micro-scale machines and the desire to reduce energy loss have drawn more attention to surface engineering methods such as creating texture and sliding on the surface. So far, little study has been done on the effect of sliding on such textured surfaces. Sing and Kango [17, 18] evaluated the combined use of micro-textures and 'wettability gradient' on the thermo-hydrodynamic performance of inclined slider bearings. In this article, a model for the possibility of fluid slippage in lubrication between a cylinder, and a surface with a dimple texture has been described, and the governing equations for fluid flow have been derived. Then, by solving the set of equations, the behavior of the lubricant under the conditions of the possibility of slippage has been modeled and the effect of different parameters has been investigated. They showed that the slip-textured bearings exhibited significant improvement in the average pressure and temperature of the lubricant.

2. Governing equations

The geometry of the contact between two non-conformal surfaces, which can lead to the elastohydrodynamic lubrication regime, is modeled as the contact between a cylinder and a flat surface. For dimpled surfaces, the flat surface is considered pitted. Figure 1 shows an elastohydrodynamic line contact of a flat surface compared to a dimpled surface. As the cylinder passes over the dimple, the contact geometry changes. The pressure distribution, film thickness variation, and the possibility of sliding on each surface is also can change as well.

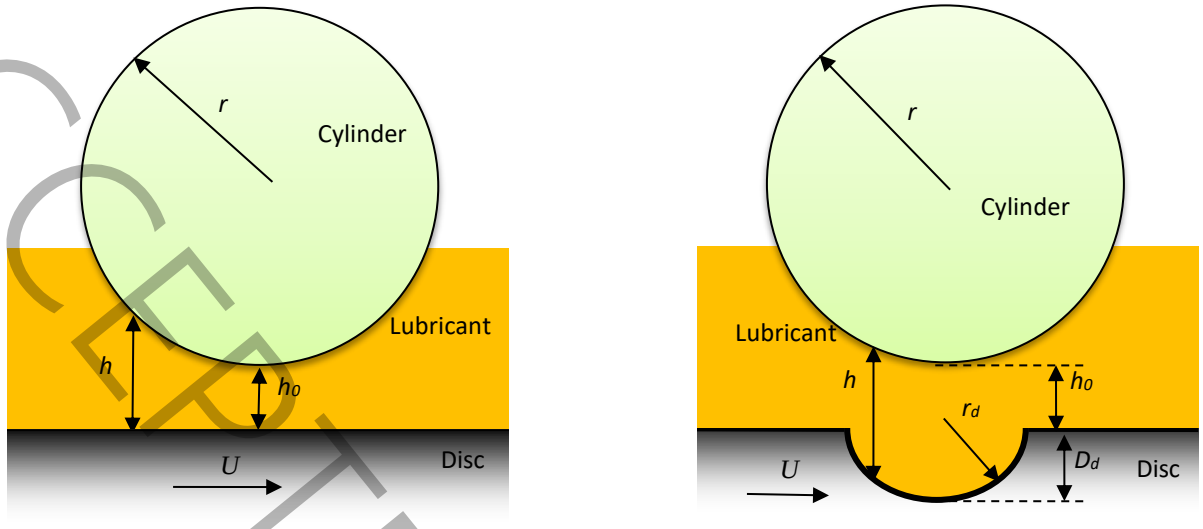

Fig. 1: Linear contact on a flat surface (left) and on a surface with a small dimple (right)

The mathematical model includes three equations: first, the modified Reynolds equation, which is derived from the Navier-Stokes, and the continuity equations by considering the boundary slip condition. It relates the pressure of the lubricant film to the lubricant film thickness, contact geometry, and surface velocities. Second, the film thickness equation, which with the assumption of being flooded condition can be expressed as the distance between two contact surfaces by considering the elastic deformation, and third, the load balance equation, which states that the total pressure produced in the lubricant film must be in balance with the total normal load. Also, due to very high pressure, lubricant properties such as viscosity and density change with the pressure, and the model is completed with the rheology equations.

2-1-The Reynolds equation

Reynolds equation is a partial differential equation governing the pressure distribution in classical lubrication theory. This equation is derived from the Navier-Stokes equation and the mass conservation equation. The standard form of Reynolds equation for the contact of a cylindrical surface with a flat surface is as follows [19]:

$$\frac{\partial}{\partial x}\left(\frac{\rho h^3}{\mu}\frac{\partial p}{\partial x}\right)=6\frac{\partial}{\partial x}\left(\rho h\left(u_1+u_2\right)\right)+\frac{\partial h}{\partial t} \tag{1}$$

where indices 1 and 2 indicate the upper and lower surfaces. To derive this equation, it is assumed that the fluid is a Newtonian fluid, the viscous forces of the fluid dominate over the inertia of the fluid, volume forces are neglected, the pressure is fixed across the fluid film, and the thickness of the fluid film is very small compared to the contact length.

2-2-Slip modeling

The boundary sliding model used in this study is known as the critical shear stress model. According to this model, boundary sliding occurs if the shear stress of the fluid-solid contact surface is equal to a critical shear stress. The critical or limit shear stress changes linearly with pressure as [20, 21]:

$$\tau_L=\tau_0+\gamma p \tag{2}$$

According to this model, for the geometry of the solution, which includes an upper surface whose velocity and shear stress are represented by an index of one, and a lower surface where the same parameters on that surface are known by an index of two, we will have [12]:

$$\left(|\tau_1|<\tau_{L1}\right),\left(|\tau_1|<\tau_{L1}\right)\rightarrow\begin{cases}u_{\text{lub}1}=u_1\\ u_{\text{lub}2}=u_2\end{cases} \tag{3}$$

$$\left(|\tau_1|\geq\tau_{L1}\right),\left(|\tau_2|<\tau_{L2}\right)\rightarrow\begin{cases}u_{\text{lub}1}=u_{\text{lub}1}^{NN}\\ u_{\text{lub}2}=u_2\end{cases} \tag{4}$$

$$\left(|\tau_1|<\tau_{L1}\right),\left(|\tau_2|\geq\tau_{L2}\right)\rightarrow\begin{cases}u_{\text{lub}1}=u_1\\ u_{\text{lub}2}=u_{\text{lub}2}^{NN}\end{cases} \tag{5}$$

$$\left(|\tau_1|\geq\tau_{L1}\right),\left(|\tau_2|\geq\tau_{L2}\right),\left(|\tau_1|<|\tau_2|\right)\rightarrow\begin{cases}u_{\text{lub}1}=u_{\text{lub}1}^{NN}\\ u_{\text{lub}2}=u_2\end{cases} \tag{6}$$

$$\left(|\tau_1| \geq \tau_{L1}\right), \left(|\tau_2| \geq \tau_{L2}\right), \left(|\tau_1| > |\tau_2|\right) \rightarrow \begin{cases} u_{lub1} = u_1 \\ u_{lub2} = u_{lub2}^{NN} \end{cases} \quad (7)$$

From the definition of shear stress for Newtonian fluid:

$$\tau_1 = -\frac{h}{2}\frac{\partial p}{\partial x} + \mu\frac{u_2 - u_1}{h} \quad (8)$$

$$\tau_2 = \frac{h}{2}\frac{\partial p}{\partial x} + \mu\frac{u_2 - u_1}{h} \quad (9)$$

that the positive direction of τ is considered against the direction of the x-axis in the lower surface (surface 1) and in the direction of the x-axis in the upper surface (surface 2). At the moment of slippage, the velocity value of the lubricant in surface 1 is obtained as:

$$u_{lub1}^{NN} = u_2 - \frac{h}{\mu}\left(\pm\tau_{L1} + \frac{h}{2}\frac{\partial p}{\partial x}\right) \quad (10)$$

And for surface 2, we will have the same way:

$$u_{lub2}^{NN} = u_1 + \frac{h}{\mu}\left(\pm\tau_{L2} - \frac{h}{2}\frac{\partial p}{\partial x}\right) \quad (11)$$

The positive or negative sign should be chosen based on the direction of τ_1 and τ_2.

2-3-Film thickness

The analysis geometry consists of two non-symmetrical surfaces consisting of a cylinder and a plate with dimple texture. According to Figure 1, the relationship for film thickness change will be as follows [22]:

$$h = h_0 + \frac{x^2}{2R} + \frac{2}{\pi E'}\int_{-\infty}^{+\infty} p\ln\left(x - x'\right)^2 dx' + Dimple \quad (12)$$

Where h_0 is minimum film thickness, the second term stands for approximating the circular shape of the cylinder, the third statement is for surface deflection, and finally

$$Dimple = \sqrt{r_d^2 - x^2} - \left(r_d - D_d\right) \tag{13}$$

2-4-Lubricant behavior modeling

It's supposed that the properties of lubricants change with pressure and temperature. When heat effects are ignored in an analysis and simple isothermal conditions are considered; The governing equations for changes in the viscosity and density of the lubricant with pressure are obtained from the reference [23] as follows:

$$\mu = \exp\left(\frac{-26.85298\left(T - T_g(p)\right)F(p)}{39.17 + \left(T - T_g(p)\right)F(p)}\right) \times 1.23e7 \tag{14}$$

$$T_g(p) = -88.69 + 263.8\ln\left(1 + 0.3527\right) \tag{15}$$

$$F(p) = \left(1 + 13.73p\right)^{-0.3426} \tag{16}$$

Density changes are small compared to viscosity changes. However, there is very high pressure in the elastohydrodynamic lubrication film and the lubricant cannot be considered as an incompressible medium; Therefore, it is necessary to consider the dependence of density on pressure. The density value in this study is obtained using the relationship known as [24]:

$$\frac{\rho}{\rho_0} = \left(1 + \frac{0.6p}{1 + 1.7p}\right) \tag{17}$$

2-5- Load equation

The vertical load applied to the contact area is bear by the pressure induced in elastohydrodynamic lubricant film. Therefore, for force balance, the integral of the pressure distribution over the contact must be equal to the vertical loading W_1. In the case of one-dimensional or linear contact, the load equation is obtained as the following equation:

$$\int_{-\infty}^{+\infty} p(x)dx = W_1 \tag{18}$$

3. Simulation

When the pressure in the lubricant film is determined, the viscosity and density of the lubricant can be calculated using equations (14) and (17). Also, the surface deflection and film thickness can be estimated using equation (12). Therefore, the first step in solving the equation set is considering an initial guess for the pressure. The Reynolds equation can be solved when the film thickness and lubricant properties are known. A new pressure distribution is obtained from the solution. This new pressure distribution is again used for new estimation of film thickness and lubricant properties after solving equations (12) to (17) by applying a suitable relaxation factor. The convergence of the pressure distribution is obtained when the overall change in pressure is very small, i.e. less than 1e-6. Due to the major changes in viscosity and density with pressure, the deformation of the surfaces can be several times larger than the minimum thickness of the lubricating layer, and as a result, these equations must be solved together to achieve the pressure distribution.

The applied load will be obtained by obtaining the pressure distribution and taking the integral of the pressure over the contact surface. This equation can be both a criterion for convergence and a tool for adjusting the next step in solving the pressure distribution. Because the initial thickness of the lubricant layer, h0, in equation (11) is chosen as a guess, the load equation, equation (18), will be used to modify the minimum film thickness.

The foregoing algorithm is used to solve the steady flow problem. Figure 2 shows passing the cylinder over a dimple in four time-steps. As seen in Figure 2, the position of the dimple relative to the cylinder can affect the flow. The flow geometry changes with time as the cylinder moves over the surface. This effect can be modeled in equations with the transient term of equation (1). In this expression, the effect of changing the film thickness compared to the previous step should be considered [25, 26]. The first time step starts on the flat surface, and in several time steps, the cylinder passes over a dimple until it reaches the flat surface again. The flowchart of the solution algorithm is shown in Figure 3.

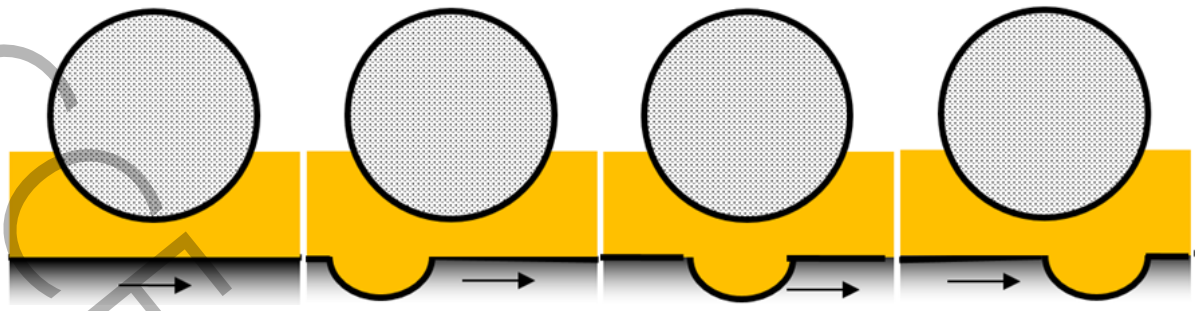

(a) First step (b) Second step (c) Third step (d) Forth step

Fig. 2: Changing the geometry of the solution when the cylinder passes over a dimple in the simulation with four time steps

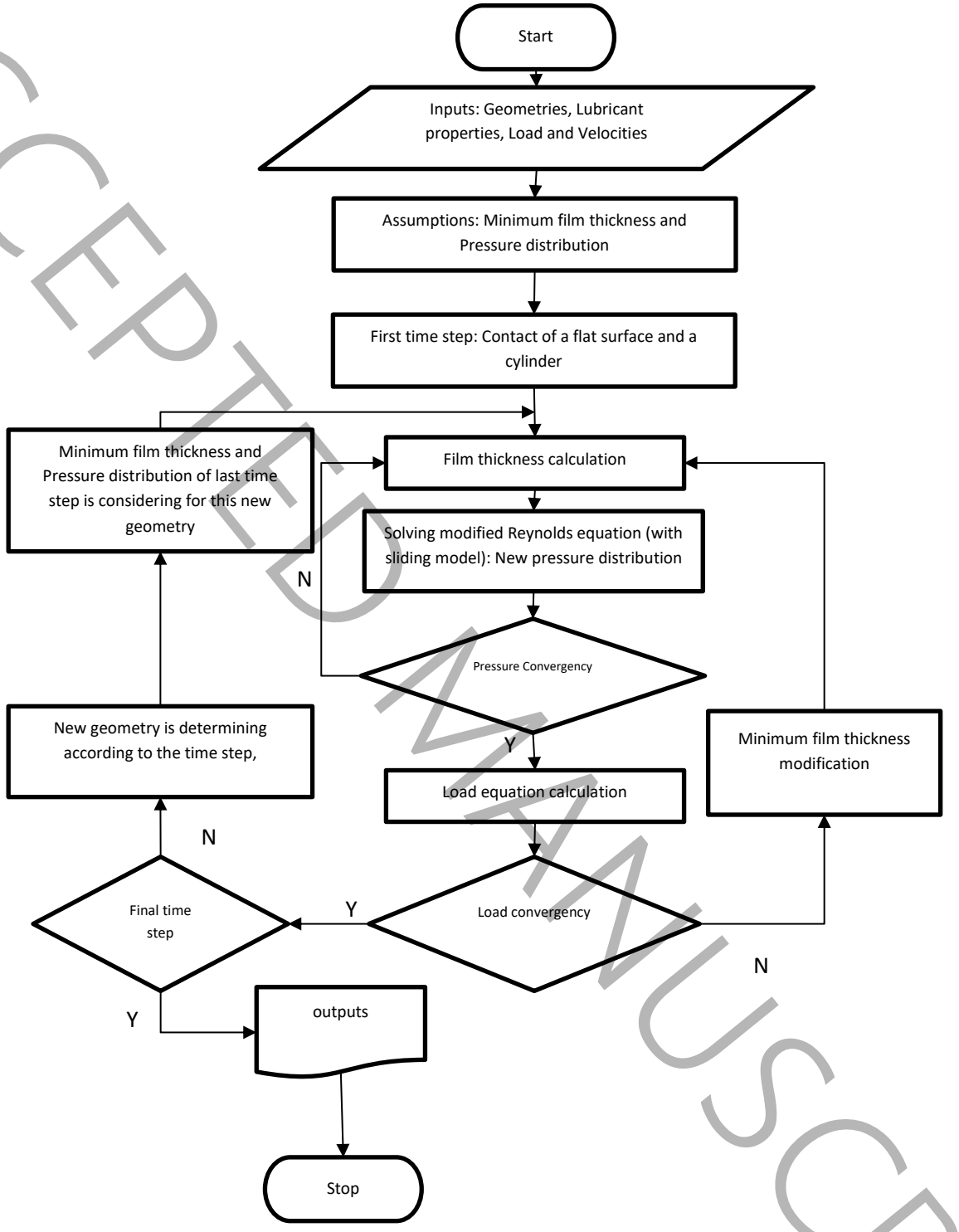

\

Fig. 3: The elastohydrodynamic problem-solving algorithm

4. Results

Choosing the appropriate dimensions of the grid elements is one of the most important steps in the numerical solution. In this research, for the proper grid size selection, the minimum thickness of the lubricating film (h_{min}), the maximum pressure (p_{max}), and the coefficient of friction (COF) were calculated for the input data listed in Table 1 based on the different number of meshes. Then the difference between each group of data has been calculated and the results are listed in Table 1.

The grid of the solution domain finer than 349 meshes does not have much effect on the lubrication parameters. Therefore, all the presented solutions have been obtained with this grid size.

Table 1: Minimum film thickness, maximum pressure, and friction coefficient in grids with different sizes

NO. Mesh	h_{min} [μm]	Diff. (%)	p_{max} [MPa]	Diff. (%)	COF	Diff. (%)
129	0.37	---	346.45	---	0.104	---
199	0.29	21.62	271.72	21.57	0.0069	33.65
249	0.28	3.57	271.53	0.07	0.0073	5.80
299	0.34	21.43	269.01	0.93	0.0059	19.18
349	0.33	2.94	268.99	0.01	0.0061	3.39
399	0.32	3.03	268.97	0.01	0.0062	1.64
449	0.32	0.00	268.96	0.00	0.0064	3.23

Comparing and measuring the numerical solution data with reliable data obtained from experiments or previous studies is essential in numerical modeling. For this purpose, to validate the data, a comparison has been made between the present results and the data of several similar research works. The research study of Stahl and Jacobson [27] which is close to the study of Jacobson and Hamrock [28] and the study of Lee and Hamrock [29] has been selected. The comparison has been made based on the geometric coordinates of the sliding range along the contact area and also on the minimum ratio of the lubricant film thickness to the radius of the equivalent radius (R). Table 2 shows the relevant comparison.

Comparison results are slightly different from each other. The slide area overlaps with the study of Stahl and Jacobson. The percentage difference in hmin/R is 28% compared to Jacobson and Hamrock's study and

15.5% with Stahl and Jacobson; in comparison with the study of Lee and Hamrock, it is 15.07% and with Stahl and Jacobson, it is 18.56%.

In this section, the results of lubrication simulation with two assumptions of slip or non-slip occurrence near the wall for various velocities, loads, and different dimensions of the dimple are presented. The solution domain range is -4≤X≤4. The geometry of flow in this type of problem varies with time and it is necessary to use the transient solution method. As shown in Figure 2, a proper step number should be chosen to model the dimple pass phenomenon. Here, the analysis has been carried out in seven time steps, which start from the first time step on a flat surface without a dimple, and then in each time step, the cylinder passes over a dimple until it finally reaches again to the flat surface.

Table 2: Comparison between the results of previous studies and the results of the current model

Study	h_{min}/R	**Slip Area**
Jacobson & Hamrock, [28]	1.8687×10^{-5}	-0.22≤X≤0.52
Stahl and Jacobson, [27]	2.0860×10^{-5}	-0.27≤X≤0.70
Present study	2.4105×10^{-5}	-0.36≤X≤0.70
Lee and Hamrock, [29]	1.2705×10^{-5}	-0.55≤X≤0.55
Stahl and Jacobson, [27]	1.3250×10^{-5}	-0.74≤X≤0.80
Present study	1.0790×10^{-5}	-0.81≤X≤0.88

The lubricant parameters and input data are given in Table 3; The varying parameters are surface speeds and amount of loading, which were studied along with the effects of the dimple depth and dimple radius. For different values of these parameters, the friction coefficient has been calculated for both slip and no-slip conditions.

Table 3: Initial input values in the lubrication on dimpled surface

Parameter	**Value**	**unit**
Dimple depth (D_d)	10	$[\mu m]$
Dimple radius (r_d)	50	$[\mu m]$
Viscosity-Pressure index (z)	0.61	$[-]$
Viscosity-Pressure constant (α)	2E-08	$[Pa^{-1}]$
Limited shear stress at ambient pressure (τ_0)	2E06	$[Pa]$

Limit shear stress proportionality factor (γ)	0.02	$[-]$
Elasticity modulus (E)	2.11E11	$[Pa]$
Poisson ration (ν)	0.3	$[-]$
Lubricant viscosity at ambient pressure (μ_0)	0.04	$[Ns/m^2]$
The sum of surface velocity: US=U_1+U_2	2.0	$[m/s]$
Ratio of surface velocity: UR=U_2/U_1	0.8	$[-]$
The curvature radius of the lower surface (R_1)	0.0170	$[m]$
The curvature radius of the upper surface (R_2)	0.1005	$[m]$
Pin width (d)	0.02	$[m]$
Load (W)	800	$[N]$

Figures 4 show the pressure distribution and Figure 5 shows the thickness of the lubricant film thickness for the working conditions listed in Table 3, in the first, third, fifth, and seventh time steps for both no-slip and slip conditions on the surface. Considering the slip condition affects the pressure and film thickness distribution. The film thickness is considerably thicker than the no-slip condition, and a lower pressure is estimated.

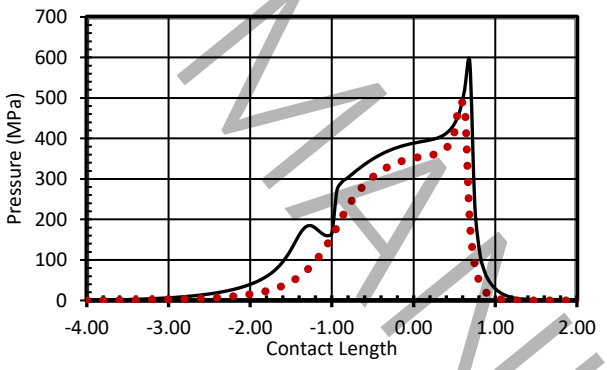

A) Step 1

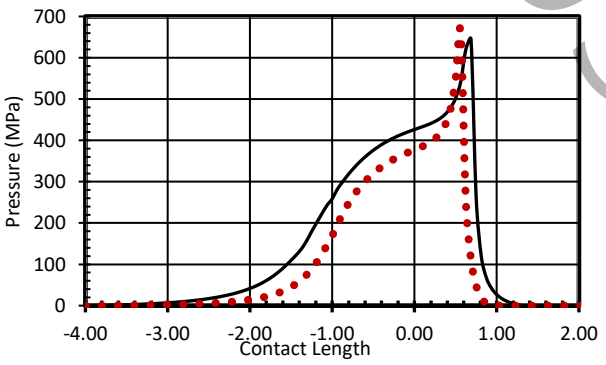

B) Step 3

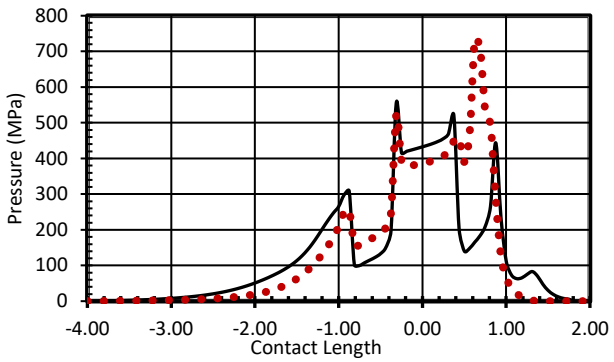

C) Step 5

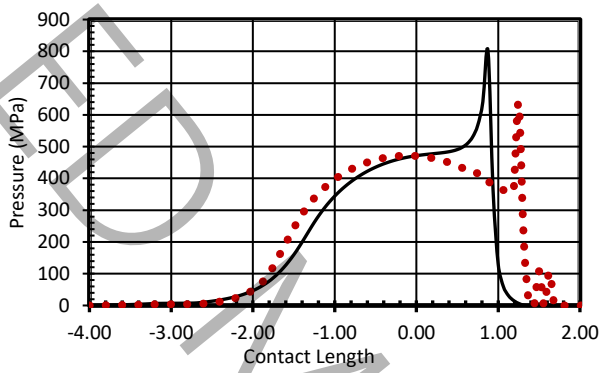

D) Step 7

Fig. 4: Pressure distribution over contact length for various time step with slip and no-slip condition

——— : Slip condition ●●● : No-slip condition

Friction along the contact surface is a practical parameter that can be used to compare the lubrication condition with and without the wall sliding assumption. The following equation is used to calculate the friction force:

$$fr = \sum_{i=1}^{N} \left(\frac{p_{i+1} - p_i}{\Delta x} \frac{h_i}{2} + \mu \frac{U}{h_i} \right) \Delta x \qquad (19)$$

The friction coefficient is also calculated as follows:

$$COF = \frac{fr}{w} \tag{20}$$

The comparison results are given in Table 4. First, the effect of the surface speed has been investigated; For this purpose, the value of friction coefficients in two cases of slip condition and no-slip condition for sliding on the wall of the contact surface has been calculated for 5 total cases of different speeds in the range of 1.5 to 3.5 m/s. The comparison of the obtained values shows that the occurrence of slip causes an average reduction of 14.30 % of the friction coefficient; That is, the occurrence of slippage can lead to an increase in lubrication efficiency by reducing the friction force.

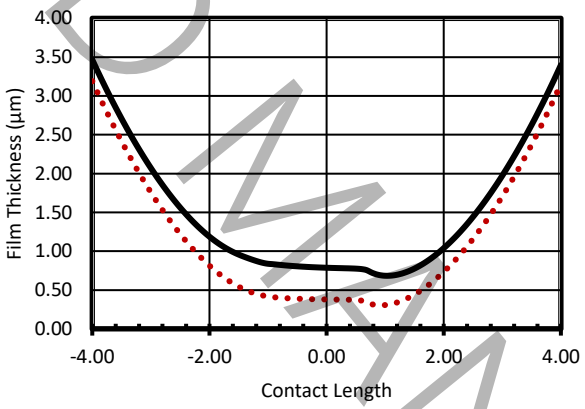

A) Step 1

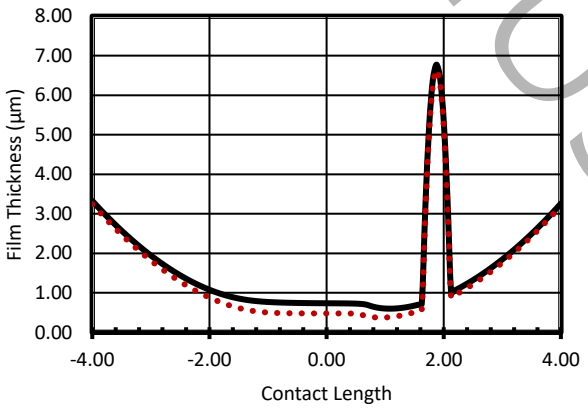

B) Step 3

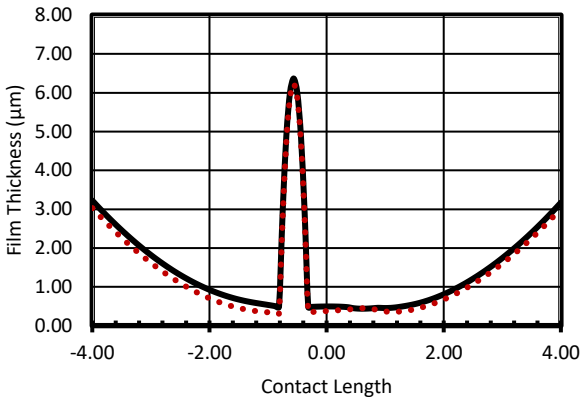

C) Step 5

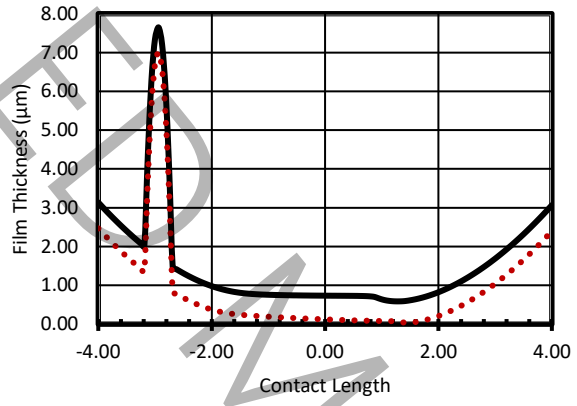

D) Step 7

Fig. 5: Lubricant film thickness distribution over contact length for various time steps with slip and no-slip condition

——— : Slip condition ●●● : No-slip condition

The comparison of friction coefficients for different loads has also shown that the friction coefficient in the case of wall sliding has a smaller value than in the case of no sliding. On average, with the occurrence of sliding in the wall, it has decreased by 10.72 %, which indicates that with the occurrence of sliding, the lubrication efficiency will increase while reducing the friction force.

Table 4: Comparison of the friction coefficient of the surface with holes, assuming the occurrence and non-occurrence of slip

Load (N)	Speed (m/s)	Geometry of Dimple (µm)	COF with slip	COF no slip	Reduction (%)

		Depth	Radi			
800	1.5	10	50	0.033	0.040	15.91
800	2.0	10	50	0.031	0.036	14.17
800	2.5	10	50	0.029	0.035	16.95
800	3.0	10	50	0.027	0.030	11.67
800	3.5	10	50	0.025	0.029	12.80
700	2.0	10	50	0.017	0.019	8.02
750	2.0	10	50	0.021	0.023	8.89
800	2.0	10	50	0.031	0.036	14.17
850	2.0	10	50	0.038	0.041	7.82
900	2.0	10	50	0.041	0.046	10.55
950	2.0	10	50	0.043	0.050	14.88
800	2.0	5	50	0.016	0.020	19.60
800	2.0	10	50	0.031	0.036	14.17
800	2.0	15	50	0.062	0.070	11.98
800	2.0	20	50	0.097	0.099	2.52
800	2.0	10	30	0.039	0.042	8.08
800	2.0	10	40	0.034	0.038	10.58
800	2.0	10	50	0.031	0.036	14.17
800	2.0	10	60	0.030	0.033	10.24

Other important factors that can be investigated are the location of the slip and the comparison between the upper and lower surface shear stress, there will be 5 conditions of slip which are defined as follows:

Condition 0: the shear stress in both surfaces is smaller than the limit shear stress of the surface and no-slip occurs;

Condition 1: slippage occurs on the lower level and the conditions for slippage are not met on the upper level;

Condition 2: the slip occurs on the upper level and the condition for the slip does not exist on the lower level;

Condition 3: the shear stress on both surfaces is greater than the limit shear stress of the surface, and the shear stress of the lower surface is greater than the shear stress of the upper surface, so it is assumed that slip occurs on the lower surface;

Condition 4: the shear stress on both surfaces is greater than the surface's limit shear stress, and the upper surface's shear stress is greater than the shear stress of the lower surface, so it is assumed that slip occurs on the upper surface.

Figures 6 and 7 show the range and condition of slippage over contact length for various loads and speed ratios, respectively. The slippage is mainly for conditions 3 and 4 and less for types 2 and 1. The range of slippage occurrence is wide for higher loads, such as for w=1200N the slippage occurs over nearly half of the contact area. The larger the velocity ratio or the closer to zero, the larger the sliding interval can be expected. The largest wall slip occurrence interval occurs for velocity ratios of 2.0 and 0.4. Also, the shortest length of the sliding interval, for a speed ratio of 1.2 is obtained which is 18% less.

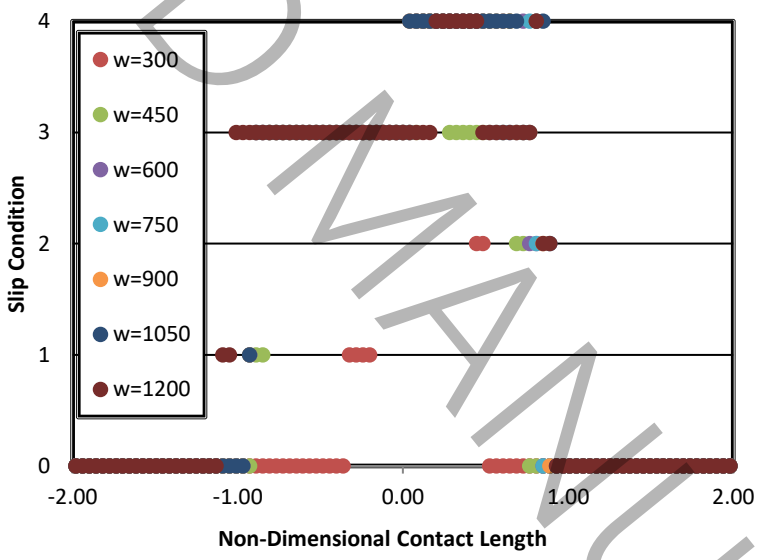

Fig. 6: The range and the condition of slips occurred for different loads

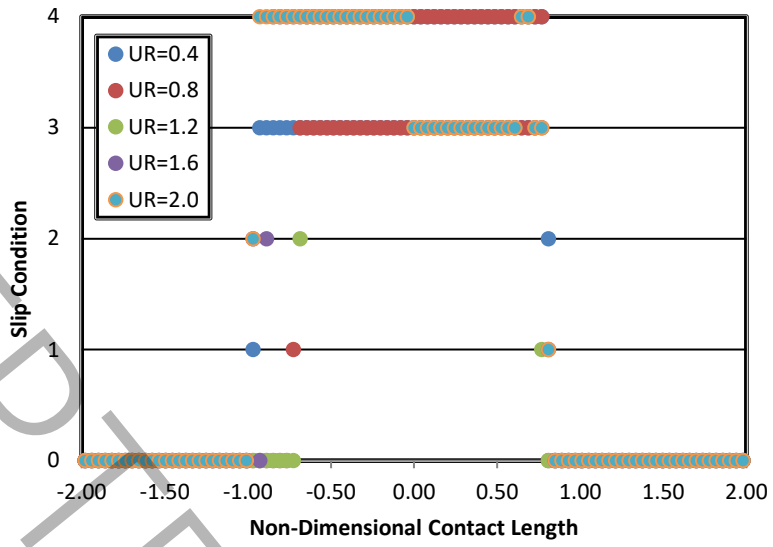

Figure 7: The range and the condition of slips occurred for different velocity ratios

5. Conclusion

After introducing critical shear stress for modeling the slippage on the surface, it is demonstrated that the occurrence of slippage has led to a decrease in the maximum pressure and the minimum thickness of the lubricant film. Fluid sliding on the surface reduces the velocity gradient on the surface and reduces the shear stress. Friction caused by fluid shear is reduced accordingly. The comparison of friction coefficients for different loads has also shown that the friction coefficient in the case of wall sliding has a smaller value than in the case of no sliding. On average, with the occurrence of sliding in the wall, it has decreased by 10.72%, which indicates the importance of sliding, the lubrication efficiency will increase while reducing the friction force.

The slip occurrence interval is larger for large or nearby zero velocity ratios. The lowest friction coefficient has been obtained for values close to one. This is probably due to the symmetry formed in the velocity field. The occurrence of slip causes an average 15.42% decrease in the friction coefficient. The difference between the maximum pressure and the minimum thickness of the lubricating film in the cases of no-slip and with slip has been negligible.

The other issues to be investigated are creating dimples with different depths and radii. In choosing the values of dimple depth and radius, the limitations of the dimple creation methods on the surface should be considered. In practice, it will not be possible to make dimples with a depth greater than the radius of the dimple. Therefore, in choosing the values of depth and radius, attention has been paid to this point. With the occurrence of slippage, the amount of friction coefficient of the surface is reduced and as a result, the amount of frictional force in the case of surface slippage is less than in the case of no slippage. With the increase in the depth of the dimple, the amount of friction coefficients increased, while the increase in the size of the radius of the dimple led to a decrease in the friction coefficient.

By comparison, the occurrence of sliding for different depths of dimples is on average 15% decrease in the amount of friction coefficient while it decreases by about 12% for different radii of the dimple. Therefore, it is possible to increase the lubrication efficiency by choosing a suitable geometry for the dimple while sliding occurs on the wall of the contact surface.

6. Nomenclature

b	Half-length of Hertzian contact, (m)	x	Coordinate, (m)
E'	Equivalent modulus of elasticity, (Pa)	X	Non-dimensional contact length (=x/b)
h	Film thickness, (m)	γ	Proportional coefficient of limited shear stress
h_0	Initial Film thickness, (m)	μ	Viscosity, (Pa.s)
i,j	Grid indexes	μ_0	Viscosity at ambient pressure, (Pa.s)
N	Size of grid	ν	Poisson Coefficient
p	Pressure, (Pa)	ρ	Density, (kg/m3)
R	Equivalent radius of curvature, (m)	ρ_0	Density at ambient pressure, (kg/m3)
U	Nondimensional velocities	$\tau_1.\tau_2$	Shear stress, (Pa)
$U_1.U_2$	Surface velocities, (m/s)	τ_0	Shear stress at ambient pressure, (Pa)
$U_{lub1}.U_{lub2}$	Lubricant velocities, (m/s)	τ_L	Limited shear stress, (Pa)
$U_{lub1}^{NN}.U_{lub2}^{NN}$	Lubricant velocities during the slippage, (m/s)		
w	Load, (N)		

7. References

[1] M. Kaneta, H. Nishikawa, K. Kameishi, Observation of wall slip in elastohydrodynamic lubrication, ASME journal of tribology, 112(3) (1990) 447-452.

[2] P. Wong, X. Li, F. Guo, Evidence of lubricant slip on steel surface in EHL contact, Tribology International, 61 (2013) 116-119.

[3] A. Ponjavic, J.S. Wong, The effect of boundary slip on elastohydrodynamic lubrication, RSC Advances, 4(40) (2014) 20821-20829.
[4] L. Guo, P. Wong, F. Guo, Correlation of contact angle hysteresis and hydrodynamic lubrication, Tribology Letters, 58 (2015) 1-9.
[5] X. Jin, J. Wang, Y. Han, N. Sun, J. Zhu, Discrepancy in oil film distribution observed in ZEV reciprocating motion, Industrial Lubrication and Tribology, 73(1) (2021) 177-189.
[6] W. Feng, Y. Han, G. Xiang, J. Wang, Hydrodynamic lubrication analysis of water-lubricated bearings with partial microgroove considering wall slip, Surface Topography: Metrology and Properties, 9(1) (2021) 015019.
[7] M. Tauviqirrahman, M.F. Afif, P. Paryanto, J. Jamari, W. Caesarendra, Investigation of the tribological performance of heterogeneous slip/no-slip journal bearing considering thermo-hydrodynamic effects, Fluids, 6(2) (2021) 48.
[8] M. Arif, S. Kango, D.K. Shukla, Investigating the effect of different slip zone locations on the lubrication performance of textured journal bearings, Industrial Lubrication and Tribology, 73(6) (2021) 872-881.
[9] M. Arif, S. Kango, D.K. Shukla, Analysis of textured journal bearing with slip boundary condition and pseudoplastic lubricants, International Journal of Mechanical Sciences, 228 (2022) 107458.
[10] B. Yao, G. Xiang, J. Wang, J. Guo, Y. Nie, Effects of wall slip on hydrodynamic performances of water-lubricated bearings under transient operating condition, International Journal of Surface Science and Engineering, 17(2) (2023) 73-91.
[11] X. Yi, H. Xu, G. Jin, Y. Lu, B. Chen, S. Xu, J. Shi, X. Fan, Boundary slip and lubrication mechanisms of organic friction modifiers with effect of surface moisture, Friction, (2024) 1-16.
[12] Y. Zhang, S. Wen, An analysis of elastohydrodynamic lubrication with limiting shear stress: part I—theory and solutions, Tribology transactions, 45(2) (2002) 135-144.
[13] F. Aurelian, M. Patrick, H. Mohamed, Wall slip effects in (elasto) hydrodynamic journal bearings, Tribology International, 44(7-8) (2011) 868-877.
[14] Q.-D. Chen, H.-C. Jao, L.-M. Chu, W.-L. Li, Effects of anisotropic slip on the elastohydrodynamic lubrication of circular contacts, Journal of Tribology, 138(3) (2016) 031502.
[15] Y. Zhao, P. Wong, L. Guo, Linear complementarity solution of 2D boundary slip EHL contact, Tribology International, 145 (2020) 106178.
[16] B. Sun, L. Chen, L. Guo, W. Wang, P. Wong, Experimental evidence on the enhancement of bearing load capacity by localised boundary slip effect, Tribology Letters, 69 (2021) 1-8.
[17] M.Y. Çam, M. Giacopini, D. Dini, L. Biancofiore, A numerical algorithm to model wall slip and cavitation in two-dimensional hydrodynamically lubricated contacts, Tribology International, 184 (2023) 108444.
[18] S. Singh, S. Kango, Effect of sliding speed on the thermohydrodynamic performance of partially slip-textured slider bearings, Lubrication Science, 35(8) (2023) 574-595.
[19] B.J. Hamrock, S.R. Schmid, B.O. Jacobson, Fundamentals of fluid film lubrication, CRC press, 2004.
[20] G. Ma, C. Wu, P. Zhou, Influence of wall slip on the hydrodynamic behavior of a two-dimensional slider bearing, Acta Mechanica Sinica, 23(6) (2007) 655-661.
[21] Z. Fu, P. Wong, F. Guo, Effect of interfacial properties on EHL under pure sliding conditions, Tribology Letters, 49 (2013) 31-38.
[22] B. Jacobson, On the lubrication of heavily loaded cylindrical surfaces considering surface deformations and solidification of the lubricant, ASME journal of tribology, 95(3) (1973) 321-327.
[23] S. Yasutomi, S. Bair, W. Winer, An application of a free volume model to lubricant rheology I—dependence of viscosity on temperature and pressure, ASME journal of tribology, 106(2) (1984) 291-302.
[24] D. Dowson, G.R. Higginson, Elasto-hydrodynamic lubrication: international series on materials science and technology, Elsevier, 2014.
[25] A. Torabi, M.H. Alidousti, Numerical and experimental study of elastohydrodynamic grease lubrication of dimple textured surfaces, Acta Mechanica, 234(7) (2023) 2919-2931.

[26] A. Torabi, S. Akbarzadeh, B. Azami, Transient numerical modeling and experimental investigation of the effect of surface texture on elastohydrodynamic lubrication, Amirkabir Journal of Mechanical Engineering, 53(5 (Special Issue)) (2021) 3201-3212.
[27] J. Sta˚ hl, B.O. Jacobson, A lubricant model considering wall-slip in EHL line contacts, J. Trib., 125(3) (2003) 523-532.
[28] B. Jacobson, B. Hamrock, Non-Newtonian fluid model incorporated into elastohydrodynamic lubrication of rectangular contacts, ASME journal of tribology, 106(2) (1984) 275-282.
[29] R.-T. Lee, B. Hamrock, A circular non-Newtonian fluid model: part I—used in elastohydrodynamic lubrication, ASME journal of tribology, 112(3) (1990) 486-495.